Monomer−Dimer Equilibrium of Normal and Modified βA3-Crystallins: Experimental Determination and Molecular Modeling

Y. V. Sergeev,*,⊥ P. T. Wingfield,|| and J. F. Hejtmancik⊥

National Eye Institute and National Institute of Arthritis and Musculoskeletal and Skin Diseases, National Institutes of Health, Bethesda, Maryland 20982

Received August 10, 2000; Revised Manuscript Received October 26, 2000

ABSTRACT: β- and γ-Crystallins are major protein constituents of the mammalian lens, where their stability and association into higher order complexes are critical for clarity and refraction. Two regions of the βγ-crystallins have been suggested to modulate protein association, namely, the flexible N-terminal extensions and the intramolecular domain interfaces. The oligomeric state of wild-type recombinant murine βA3-crystallin (rβA3) was compared to that of modified βA3-crystallins with either an N-terminal deletion of residues 1 to 29 (rβA3tr) or with residues 114 to 123 of the interdomain linker replaced with the analogous linker from murine γB-crystallin (rβA3cp). All three proteins exhibited reversible monomer−dimer formation. The modifications to the N-terminus and domain linker resulted in tighter dimer formation as compared to wild-type protein as indicated by disassociation constants determined by sedimentation equilibrium: 6.62×10^{-6} M (rβA3), 0.86×10^{-6} M (rβA3cp), and 1.83×10^{-7} M (rβA3tr). Homology modeling of βA3-crystallins and solvation energy calculations also predicted tighter binding of the modified crystallins consistent with the centrifugation results. The findings suggest that under physiological conditions βA3 crystallin exists in a dynamic equilibrium between monomeric and dimeric protein and that modification, especially to the N-terminal extension, can promote self-association.

Crystallins make up over 90% of the water-soluble protein of the mammalian eye lens, where they are critical for lens transparency and refraction. In the vertebrate eye lens, three major classes of ubiquitous crystallins are found: α-, β-, and γ-crystallins (*1, 2*). The β- and γ-crystallins have a common polypeptide chain fold, share conserved sequences, and together form a superfamily of βγ-crystallins (*3*). In contrast, the α-crystallins form a separate family of proteins related to the small heat-shock proteins (*4*). Mutations in βγ-crystallin genes can lead to nonspecific aggregation of the βγ-crystallins resulting in cataract formation (*5*−*12*) as can mutations that alter γD-crystallin association without changing the polypeptide chain fold (*13, 14*).

βγ-Crystallins comprise two domains connected by an 8−10 amino acid interdomain linker. Each domain has an identical polypeptide chain fold, namely, a β-sandwich of two antiparallel β-sheets, known as a "Greek key" motif (*15*−*19*). The relative position of the two domains in γB- and βB2-crystallins differ, having either "closed" or "opened" conformations, respectively (*20*). The surface location of the interdomain interface in both bovine γB and βB2 is very similar (*19, 21*). However, in monomeric γB, intramolecular domains form the interface, whereas in homodimeric βB2, the interface consists of residues from the N-terminal domain of one monomer and residues from the C-terminal domain of the second monomer in a switched domain fashion. The physical properties of β-sheet residues forming the interdomain interface in βA3 crystallin (βA3) are similar to those in γB and βB2, especially those residues showing significant accessibility changes upon formation of the interface (*22*). This suggests that the conserved layer structure of the interface may be important for dimer formation. The similarity of the domain docking sites may also explain subunit exchange between homo- and heterodimers of the βA3 and βB2 (*22*).

The study of crystallin mutants in human cataracts and animal models provides insight into those regions of the β-crystallin molecule important for protein association. The terminal extensions are such regions where specific mutations or deletions can modulate protein association (*23*). In bovine βB2, the removal of residues at the N-terminus or the C-terminus does not inhibit dimerization (*24*). The N-terminal extension (residues 1−22) in homodimeric bovine βA3 is both flexible and exposed to solvent (*25*). Truncation of the N-terminal extension appears to affect dimerization as assessed by gel filtration (*26*). Also, insertion of the bovine γB-linker into βB2-crystallin, thus, replacing the normal linker, results in monomer formation (*27*). In contrast, insertion of the γB linker into the murine βA3 does not inhibit dimer formation (*28*), and bovine γB with βB2-linker inserted is still monomeric (*20*).

To further investigate the importance of the amino-terminal extension and connecting peptide for the stability of β-crystallin complexes, the oligomeric state of wild-type rβA3-crystallin was studied and compared to mutants with either

* To whom correspondence should be addressed. Yuri V. Sergeev, OGVFB/NEI/NIH, 10/10B10, 9000 Rockville Pike, Bethesda, MD 20892; Telephone: 301-594-7053: Fax: 301-435-1598; E-mail: sergeev@helix.nih.gov.

⊥ National Eye Institute.

|| National Institute of Arthritis and Musculoskeletal and Skin Diseases.

10.1021/bi001882h
Published on Web 12/01/2000

an N-terminal deletion (rβA3tr) or one where residues 114 to 123 of the interdomain linker were replaced with the analogous linker from γB-crystallin (rβA3cp). Under our experimental conditions, all recombinant βA3 proteins appear to conform physically to reversible monomer−dimer equilibrium systems with K_d (rβA3) > K_d (rβA3cp) > K_d (rβA3tr). Three-dimensional structures of recombinant crystallins were each modeled as "opened" and "closed" monomers or as a dimer. Solvation free energies were calculated for each model, and the results were consistent with the sedimentation equilibrium data, predicting tighter binding constants for the βA3cp and βA3tr dimers as compared to wild-type protein.

MATERIALS AND METHODS

Protein Expression and Purification. Wild-type and modified recombinant murine βA3-crystallins were prepared as previously described (*26*, *28*). In rβA3tr, N-terminal residues 1−29 were removed and residue 30 was mutated (W30G). In rβA3cp, the 10-residue connecting sequence PICSANHKES (residues from Pro 114 to Ser 123) was replaced with the 9-residue sequence LIPQHSGTY from murine γB. The recombinant proteins rβA3, rβA3cp, and rβA3tr were all purified as briefly described below. Infected insect cells were lysed by freeze thawing in 1 mL of buffer A: 50 mM Tris-HCl,[1] pH 8.5, 1 mM EDTA, and 1 mM DTT. The lysates were centrifuged at 10600*g* for 30 min at 4 °C, and the supernatants were dialyzed overnight against 2 L of buffer A containing E-64 Cys protease inhibitor (Boehringer Manniheim GmbH). Proteins were purified at room temperature using a FPLC Bio-Logic workstation (Bio-Rad). Soluble extracts were loaded onto a 6-mL DE-52 column (Whatman) equilibrated with buffer A and eluted at a flow rate of 0.5 mL/min. A gradient of 0−500 mM NaCl was applied, and 5 mL fractions were collected. Proteins were further purified by gel-filtration using a 124-mL Pharmacia Superdex 75 16/60 column (Pharmacia Biotech) equilibrated with buffer B: 50 mM Tris-HCl, pH 7.5, 1 mM EDTA, 1 mM DTT, and 150 mM NaCl. Samples (2 mL) were loaded on the column at a flow rate of 0.5 mL/min, and 1 mL fractions were collected. The location of recombinant proteins in the various column fractions was monitored by $A_{280\ nm}$ and by SDS−PAGE using 12% polyacrylamide gels (*29*). Protein identity was confirmed by Western blot analysis using antisera raised in rabbit against a synthetic peptide corresponding to residues 36−68 of murine βA3 (*30*).

Gel-Filtration Chromatography. Analytical gel-filtration was performed in buffer C: 50 mM Tris-HCl, pH 7.2, 1 mM EDTA, 1 mM DTT, and 150 mM NaCl using a 30-mL Superdex 75 HR 10/30 column (Pharmacia Biotech). Fractions (0.5-mL) were collected, and the flow rate was 0.5 mL/min. The column was precalibrated with low-molecular weight standards: bovine serum albumin, ovalbumin, carbonic anhydrase, chymotrypsinogen, cytochrome *c*, ribonuclease A, and aprotinin (Pharmacia, Sigma). The void and included volumes of the column were determined with Blue Dextran 2000 and 50% acetone, respectively.

[1] Abbreviations: DTT, dithiothreitol; EDTA, ethylendiaminetetraacetic acid; Tris, tris(hydroxymethyl) aminoethane; TCEP, tris(2-carboxyethyl) phosphine hydrochloride; SDS, sodium dodecyl sulfate; PDB, Protein Data Bank.

Table 1: Molecular Weights of Recombinant BA3 Crystallins[a]

β-crystallin	calc M_r (kDa)	SDS−PAGE M_r (kDa)	gel filtration M_r (kDa)	analytical ultracentrifugation M_r (kDa)	analytical ultracentrifugation K_d ($\times 10^{-6}$) (M)
rβA3	25.08	25 (± 0.5)	40 (± 3.5)	39 (± 3)	6.62 (± 2.0)
rβA3tr	21.81	23 (± 0.2)	23 (± 2.0)	40 (± 3)	0.18 (± 0.3)
rβA3cp	25.01	25 (± 0.4)	42 (± 3.7)	43 (± 3)	0.86 (± 0.3)

[a] The calculated molecular weights (M_r) were derived from protein sequences. Molecular weights were experimentally determined by SDS−PAGE, gel filtration, and analytical ultracentrifugation as described in Material and Methods section. Dissociation constants (K_d) were determined from sedimentation equilibrium using a monomer−dimer model to fit to concentration profiles (see Materials and Methods). Values in parentheses are the standard errors. Analytical ultracentrifugation data assume that standard error for each data point are equal to the square root of the χ^2-values.

Analytical Ultracentrifugation. Only those samples showing a single peak on analytical gel-filtration columns and that were greater than 95% pure as judged by SDS−PAGE were used. To minimize artifactual association of proteins due to sulfhydryl oxidation, samples were incubated for 1 h at room temperature in buffer C containing 10 mM DTT and 1.5 M urea, followed by dialysis for 24−48 h against 2 L of buffer B alone. For the analysis of rβA3cp, 50 μM of the reducing agent Tris[2-carboxyethyl]-phosphine (TCEP from Pierce) was also added to the dialyzed sample immediately prior to use. Analytical ultracentrifugation was carried out using a Beckman Optima XL-I analytical ultracentrifuge. Absorption optics, an An-60 Ti rotor, and standard double-sector centerpiece cells were used. Equilibrium measurements on the recombinant proteins at 20 °C were made after 16−20 h at 16 500 rpm. Baselines were established by overspeeding at 45 000 rpm for 4 h. Data (the average of five scans collected using a radial step size of 0.001 cm) were analyzed using the standard Optima XL-I data analysis software. Protein partial specific volumes were calculated from amino acid compositions (*31*). Values of 0.717, 0.715, and 0.718 mL/g were used for rβA3, rβA3tr, and rβA3cp, respectively. Solvent density was estimated as previously described (*32*). For the calculation of the dissociation constants (K_d), of rβA3, rβA3tr, and rβA3cp, monomeric molecular weights (see Table 1) and molar extinction coefficients of 65.82, 60.12, and 67.14 $mM^{-1}cm^{-1}$ were used, respectively.

Molecular Modeling and Energy Calculations. The structural coordinates of bovine γB (PDB: 1gcs) and βB2 (PDB: 1blb) were from the Brookhaven Protein Data Bank (*33*). The primary sequences of murine rβA3 (*34*), and bovine γB and βB2 were aligned by the method of Needleman & Wunch (*35*), incorporated in the program Look, version 3.5.2 (Molecular Applications Group). Sequence homology was used for structure modeling of monomers and dimers of rβA3. Monomers were modeled in the "closed" and "opened" forms, the former using the structure of the bovine γB monomer and the latter using the dimer of bovine βB2. Dimeric rβA3 was modeled using the structure of the bovine βB2-crystallin dimer. The "closed" monomer and dimer of the murine rβA3 were built using the automatic segment matching method in the program Look (*36*). Structures of rβA3tr and rβA3cp were mutated in a fashion similar to that described above (see Material and Methods). N-terminal

residues 1−29 were removed from the βA3 PDB data file, and residue 30 in rβA3tr file was mutated (W30G) using the model mutant procedure in Look. The initial model for rβA3cp mutant was built by replacing the 10-residue connecting sequence PICSANHKES (residues from Pro 114 to Ser 123) with the 9-residue sequence LIPQHSGTY from murine γB using the same procedure. In the rβA3tr and rβA3cp models, the conformation of the replaced residues was refined by self-consistent ensemble optimization (*37*), which applies the statistical mechanical mean-force approximation iteratively to achieve the global energy minimum structure. Finally, the predicted structures were regularized by an energy minimization procedure (Insight II, Molecular Simulations), and the geometry of all predicted structures was tested using the program Procheck (*38*).

The changes in intermolecular interactions due to amino acid residue transfer from the nonpolar environment of the protein interface to an aqueous environment were calculated from the atomic coordinates for each predicted protein model using atomic solvation energies. Solvation free energy calculations used the product of atomic solvation parameters (ASP) and accessibility of polar and apolar atoms to the solvent (*39*). Apolar and polar solvation energy terms were calculated separately for each protein molecule. Atomic solvation parameters in Kcal/A^2 units were 0.011637 for nonpolar and −0.00927 for polar atoms, 0.02241 for sulfur, −0.03753 for charged O, and −0.03695 for charged N. Accessible areas of each atom in the predicted β-crystallin structures were calculated by using analytical equations for overlapping spheres using the program Anarea (*40*).

As the conformation of the rβA3 monomer is unknown, we assumed that the βγ-crystallin domains have stable globular structures and that the conformation of monomer in solution is determined by the interdomain linker flexibility. However, as it is difficult to estimate energies for potential conformations, we assumed that monomer conformations in solution are separated into two groups: "closed" and activated "opened". These correspond to monomers with or without contact between globular domains within the same molecule. A single "opened" monomer may form a stable "closed" monomer, or two monomers in the "opened" conformation may form a stable dimer. The dissociation free energy change was derived using predicted conformations of the "closed" monomer and a dimer. Interaction free energy $\Delta G_{\text{interaction}}$ estimated by calculation the changes of solvation energy due to forming the dimer as

$$\Delta G_{\text{interaction}} = 2\Delta G_{\text{closed}} - \Delta G_{\text{dimer}}. \qquad (1)$$

Here, ΔG_{closed} and ΔG_{dimer} stand for interaction free energy of formation of the monomer in the "closed" conformation and of the dimer, respectively. Apolar and polar solvation free energy terms were estimated separately using formula 1 and combined together as previously suggested (*41*). Finally, the dissociation free energy was calculated as: $\Delta G_{\text{d}} = \Delta G_{\text{interaction}} - \Delta G_{\text{r−t}}$. Here $\Delta G_{\text{r−t}} = -T\Delta S_{\text{r−t}}$, the free energy change due to rotation and translation calculated by assuming that the same surface atoms are restricted to motions of about 1 Å (*42*). All other terms in the free energy of formation were discounted, assuming that they remain unchanged in the closed monomer and dimer.

RESULTS

Monomer−Dimer Equilibrium. The molecular weight of rβA3-crystallin was determined using gel filtration and sedimentation equilibrium (Table 1). As compared to the molecular weight predicted from the sequence or that estimated under denaturing conditions by SDS−PAGE (both ∼25 kDa), the native molecular weights determined by both gel-filtration (Figure 1, panel A) and sedimentation equilibrium (Figure 2, panel A) suggests the formation of dimeric protein (Table 1). However, as these apparent molecular weights are less than expected for a stable or tightly associated dimer, a monomer−dimer equilibrium was suspected. With the centrifugation data, diagnostic graphs of the average molecular weight as a function of protein concentration were plotted. The estimated average molecular weight systematically increases with increasing protein concentration, approaching the calculated dimer molecular weight at the bottom of the analytical cell (data not shown). Hence, application of a monomer−dimer model to the equilibrium data was applied (Figure 2). The hallmark of a good fit is where the residuals (top panels of Figure 2) from the model scatter randomly around the zero value. This is the case for the unmodified protein rβA3 and mutant rβA3cp (Figure 2, panels a and c), whereas the mutant rβA3tr shows a slight systematic downward trend near the bottom of the cell (Figure 2, panel b). This is most likely due to the presence of higher order aggregates. Attempts to obtain better fits (lower χ^2-statistics) using other models, for example, monomer−dimer−trimer, and monomer−dimer−tetramer, all resulted in significantly worse fits.

The equilibrium constant (K_{d}) for rβA3 was calculated to be 6.62×10^{-6} M, predicting that, for example, at 1 mg/mL, 75% of the protein is dimeric. The rβA3cp and rβA3tr mutants of βA3-crystallin were also treated as monomer−dimer systems (Figure 2, panels b and c). In both cases, the K_{d} values are lower, indicating tighter dimer formation (Table 1). For example, at 1 mg/mL, 92% (βA3cp) and 97% (βA3tr) of these proteins are predicted to be dimeric.

The apparent molecular weights determined using Superdex 75 gel filtration are in agreement with centrifugation data except for the βA3tr protein, which elutes with an apparent molecular mass of 23 kDa, similar to that expected for a monomer (Figure 1, panel b, Table 1). Moreover, based on the K_{d} value determined by centrifugation, even at the low protein concentrations used for gel filtration, for example ∼0.1 mg/mL, over 80% of the protein is still predicted to be dimeric (this apparent discrepancy is discussed later).

It is important to note that one of the main problems in obtaining consistent molecular weights with all three βA3 crystallins, especially by sedimentation equilibrium, is the artifactual formation of intermolecular disulfide bonds. For example, in samples not carefully reduced as described (Material and Methods), it is common to see tetramer formation, with weight average molecular masses approaching 100 kDa (data not shown). To prevent such artifacts, we have used the newly introduced reducing agent TCEP (Pierce) that has the advantages of being a better reductant than DTT and is resistant to oxidation by air and does not contribute to protein absorbance at 280 or 290 nm (unlike oxidized DTT), which can interfere with baseline calculations.

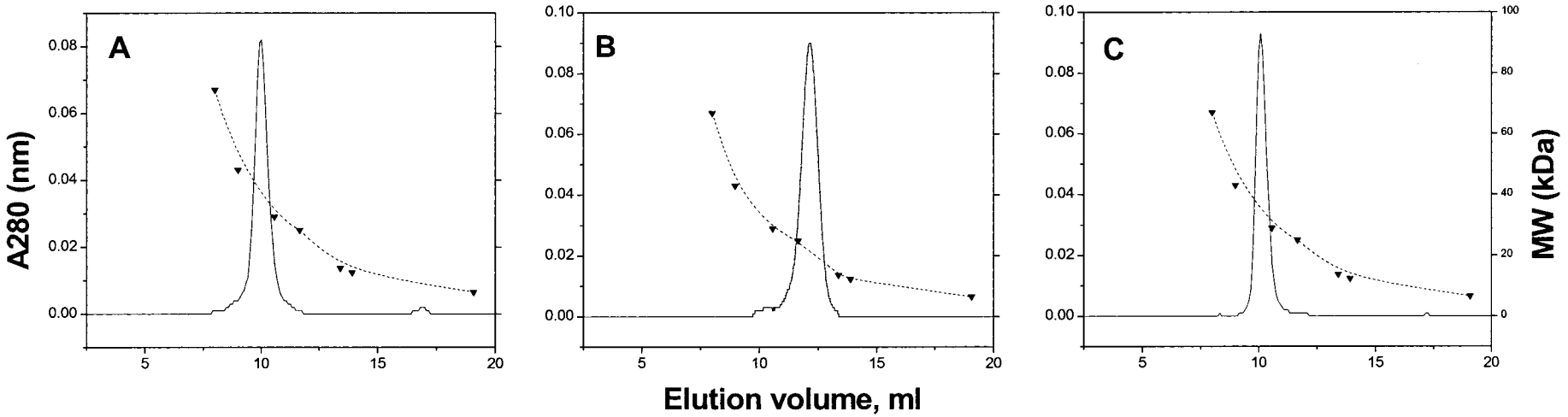

FIGURE 1: Superdex 75 10/30 HR gel-filtration chromatography of rβA3 (A), rβA3tr (B), and rβA3cp (C) as indicated by solid lines. Calibration curves for molecular weight (broken lines) are also indicated.

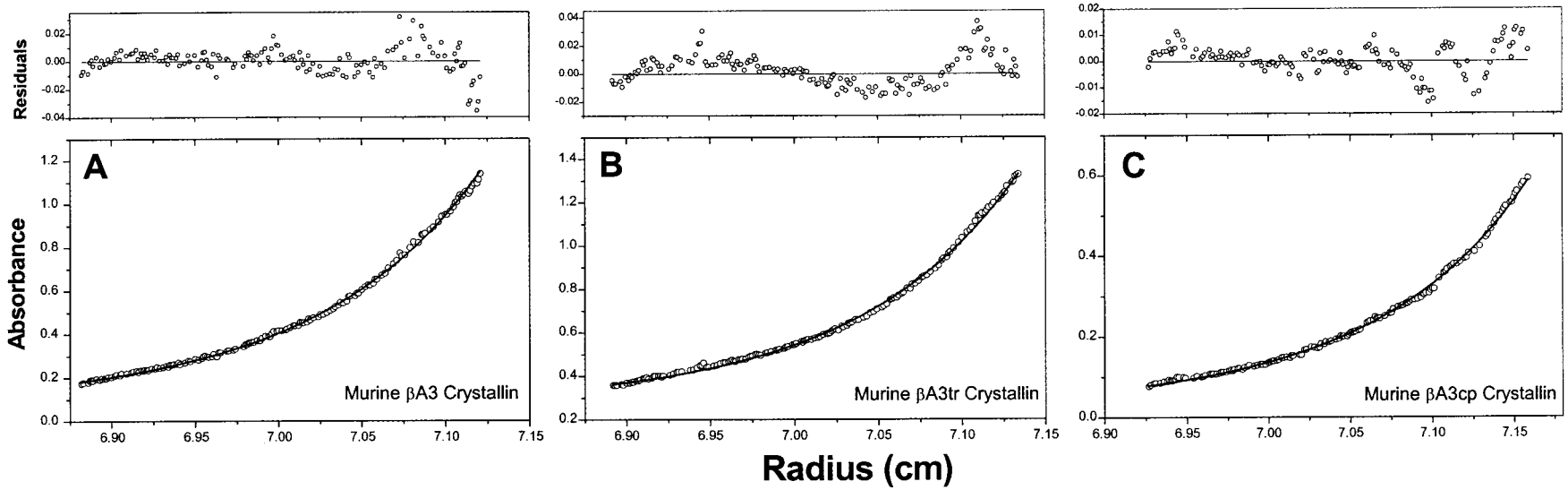

FIGURE 2: Sedimentation equilibrium data obtained for rβA3, rβA3tr, and rβA3cp. Panels are absorbance (bottom panel) and residuals (upper panel) plots for rβA3 (A), rβA3tr (B), and rβA3cp (C), respectively. Opened circles show UV absorbance gradients in the centrifuge cell. The solid line indicates the calculated fit for the monomer−dimer association. Residuals show the difference in the fitted and experimental values as a function of radial position. The χ^2-statistics for the fits shown are 5×10^{-5}, 9×10^{-5}, and 2×10^{-5}. The dissociation constants (K_d) calculated from these plots are shown in Table 1 caption.

```
betaB2   ------------ASNHETQAGKFQP--LNP-KIIIFEQENFQGHSHELNGPCPNLKETGV
gammaB   ----------------------------GKITFYEDRGFQGHCYECSSDCPNLQPY-F
betaA3   ETQTVQRELETLPTTKMAQTN-PMPGSLGPWKITIYDQENFQGKRMEFTSSCPNVSERNF
         1.......10........20........30........40........50.........

betaB2   EKAGSVLVQAGPWVGYEQANCKGEQFVFEKGEYPRWDSWTSS--RRTDSLSSLRPIK-VD
gammaB   SRCNSIRVDSGCWMLYERPNYQGHQYFLRRGDYPDYQQWMGFN----DSIRSCRLIP-QH
betaA3   DNVRSLKVECGAWIGYEHTSFCGQQFILERGEYPRWDAWSGSNAYHIERLMSFRPICSAN
         61.......70........80........90........100.......110........

betaB2   SQEHKITLYENPNFTGKKMEVIDDDVPSFHAHG-YQEKVSSVRVQSGTWVGYQYPGYRGL
gammaB   TGTFRMRIYERDDFRGQMSEITDD-CPSLQDRF-HLTEVHSLNVLEGSWVLYEMPSYRGR
betaA3   HKESKITIFEKENFIGRQWEICDD-YPSLQAMGWFNNEVGSMKIQCGAWVCYQYPGYRGY
         121......130.......140.......150.......160.......170........

betaB2   QYLLE----KGDYKDSGDFG--APQPQVQSVRRIRDMQWHQRGAFHPSS
gammaB   QYLLR----PGEYRRYLDWG--AMNAKVGSLRRVMDFY----------
betaA3   QYILECDHHGGDYKHWPEWGSHAQTSQIQSIRRIQQ------------
         181......190.......200.......210.......220.......
```

FIGURE 3: Clustal W multiple sequence alignment of the murine rβA3 and bovine γB and βB2 crystallins. Identical amino acid residues and residues with similar properties are selected using black or gray background, respectively. This alignment has been used to build predicted structures of rβA3, rβA3tr, and rβA3cp. Three-dimensional structures of bovine γB and βB2 crystallins were used as structural templates.

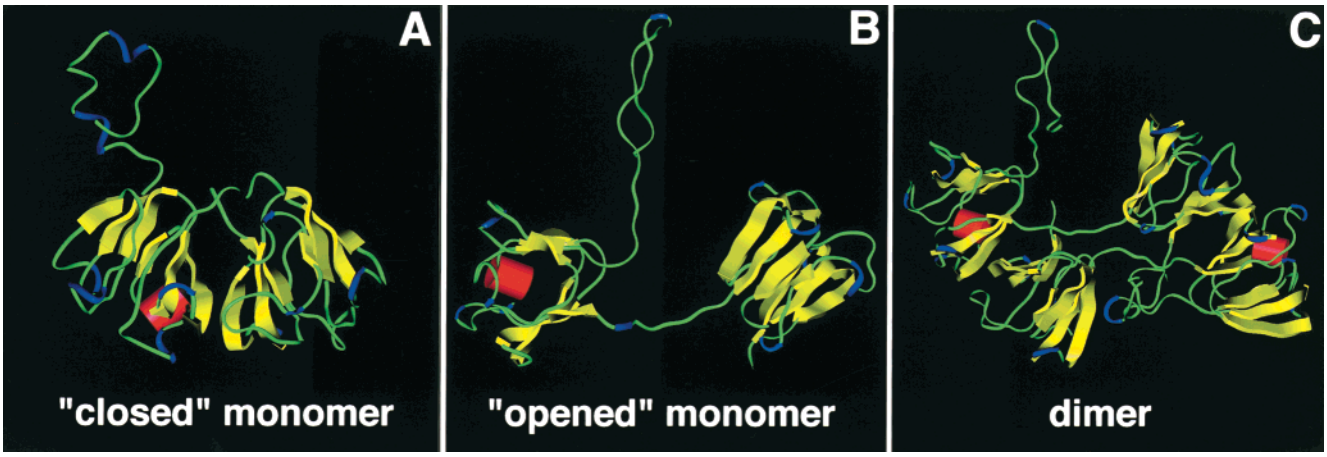

FIGURE 4: Three-dimensional structure of rβA3 obtained by homology modeling. Panels A and B indicate the "closed" and "opened" forms of the rβA3 monomer; Panel C represents the rβA3 dimer. Yellow ribbons symbolize β-sheet secondary structure and connecting loops are shown by thin green wire. Red cylinders show helices, and blue ribbon shows turns. The rβA3 dimer domains were modeled using the bovine βB2 structure (PDB: 1blb). Structures were visualized with the program Insight II, version 98.

Molecular Modeling and Energy Calculations. The multiple sequence alignments of murine rβA3, bovine γB, and βB2, chosen as the templates for structure building, are shown in Figure 3. The murine rβA3 and bovine γB sequences have an overall 38% identity and 61% similarity for common residues (Figure 3). Similarly, murine rβA3 is also closely related to bovine βB2, showing 45% identity and 62% similarity (Figure 3). Monomers in the "closed" and "opened" conformations were built using sequence homology and the known 3-dimensional structures of the bovine γB and βB2 (Figure 4). The structure of the "closed" monomer is the most compact and is modeled similarly to the bovine γB structure. The structure of the "opened" monomer is derived from the dimer of rβA3. C_α atoms in the structure of "closed" and "opened" monomers fitted their correspondent structural templates with root-mean square (rms) deviations of 0.962 and 1.383 Å, respectively. The interdomain interface of the rβA3 dimer was modeled similarly to that in the bovine βB2 structure as both proteins have similar physical properties with respect to surface residues involved in the interdomain interface (*22*). In the X-ray structure of βB2 (see PDB: 1blb), about eight residues are missing at the N-terminus and the visible parts of the terminal extensions show no similarity to those of rβA3 (Figure 4). Therefore, the amino-terminal extension of rβA3 was modeled by automatic segment matching and energy minimization combined with the predicted microdomain structure derived from proteolytic digestion studies (*43*).

Modeled rβA3 structures of "closed", "opened" monomers, and dimer are shown in Figure 4, panels a, b, and c. The predicted protein structures share a similar organization containing two domains linked with a connecting peptide and amino-terminal extensions. Although structures of "opened" and "closed" monomers of rβA3 have similar domain structures, they differ in that the connecting peptide linking the N- and C-terminal domains has either an extended or bent conformation. The dimer structure consists of two monomers having extended interdomain linkers. Each globular domain has a two-fold symmetry and a similar folding pattern that consists of the double "Greek key" motif that comprises a double β-sheet sandwich structure, similar to that found in bovine γB and βB2 (*15*, *18*). Mutant protein

Table 2: Accessible Area Changes in the Domain-Binding Interface for Recombinant βA3-Crystallins[a]

protein	monomer $\Delta A_{close-open}$	dimer formation[o] $\Delta A_{dimer-open}$	dimer formation[c] $\Delta A_{dimer-close}$
rβA3 (βA3tr)	2513 ($\pm$ 285)	4296 ($\pm$ 404)	730 ($\pm$ 342)
rβA3cp	2532 ($\pm$ 195)	4337 ($\pm$ 451)	726 ($\pm$ 405)

[a] Monomer refers to the transition between open and closed conformations. Dimer[o] refers to the association of monomers in open conformation, and Dimer[c] refers to association in the closed conformation. The area changes were determined: $\Delta A_{close-open} = A_{close} - A_{open}$; $\Delta A_{dimer-open} = A_{dimer} - 2A_{open}$, and $\Delta A_{dimer-close} = A_{dimer} - 2A_{close}$, where A_{close}, A_{open}, and A_{dimer} are the accessible areas of monomers in the "closed" and "opened" conformations and of the dimer, respectively. Changes for rβA3 and βA3tr were the same. All values are in Å^2. Values in parentheses are the standard errors. Standard errors for theoretical models were derived from structures obtained using different templates for closed monomer (PDB: 1amm, 1elp, 1a5d, and 1gcs) and for two dimers (PDB: 1blb).

Table 3: Dissociation Free Energy Changes for the Monomer−Dimer Equilibrium Calculated from the Predicted Atomic Structures of βA3-Crystallins[a]

protein	$\Delta G_{interaction}$	ΔG_{r-t}	ΔG_d calc	ΔG_d obs
βA3	16.2 ($\pm$ 4.3)	10.2 ($\pm$ 1.6)	6.0 ($\pm$ 4.5)	7.2 ($\pm$ 0.1)
βA3tr	19.6 ($\pm$ 4.3)	9.8 ($\pm$ 1.6)	9.8 ($\pm$ 4.5)	9.3 ($\pm$ 0.4)
βA3cp	19.0 ($\pm$ 3.9)	10.2 ($\pm$ 1.8)	8.8 ($\pm$ 4.3)	8.4 ($\pm$ 0.1)

[a] Energy terms are given in kcal/mol units. Here $\Delta G_{interaction}$ are interaction free energy changes calculated using apolar (ΔG_{apol}) and polar (ΔG_{pol}) solvation free energy terms in the formula $\Delta G_{interaction} = 1.4\Delta G_{apol} - 1.2\Delta G_{pol}$ as suggested by Horton and Lewis (*41*); ΔG_{r-t} are free energy changes due to entropy of rotation and translation. These terms were calculated according to ref *42*, using molecular radii determined from protein models. Calculated dissociation energy ΔG_d obtained as the difference between interaction energy $\Delta G_{interaction}$ and the energy loss due to rotation and translation ΔG_{r-t}. The experimental dissociation constants are shown in the Table 1. Observed dissociation energy ΔG_d was determined using dissociation constants K_d, where $\Delta G_d = -RT\ln K_d$ in the standard state. Values in parentheses are the standard errors. Standard errors for theoretical models were derived from structures obtained using different templates for closed monomer (PDB: 1amm, 1elp, 1a5d and 1gcs) and for two dimers (PDB: 1blb).

structures rβA3tr and the rβA3cp demonstrate rms differences in positions of C_α atoms of 0.545 and 1.172 Å for "closed" and "opened" structures, respectively. The structures of both proteins closely resemble that of βA3, and therefore, are not shown separately.

Areas of the protein surface excluded from interaction with water molecules are compared for rβA3 and the two mutant proteins to estimate hydrophobic energy changes due to dimer formation. To avoid differences in accessible areas related to different conformations of terminal extensions in the "closed" monomer and dimer, we considered only changes in interdomain interface. Excluded areas are calculated as differences between accessible areas of monomers in the "closed" or dimer conformations and the "opened" monomer conformations. For the "closed" monomeric form of rβA3 (or rβA3tr), the total change of accessible area is 2513 Å^2, whereas, for the rβA3 (or rβA3tr) dimer, this change is 4296 Å^2. The smallest area change (730 Å^2) is observed for dimer formation from the "closed" form of rβA3 (or rβA3tr). Similar changes are observed for the transitions involving rβA3cp. These results (Table 2) indicate that for all three proteins, dissociation of dimers to "closed" monomers is accompanied by less change in the accessible protein surface area and hydrophobic free energy than formation of an "opened" monomer. As a result, surrounding water molecules will gain less entropy, consistent with stable conformations for the "closed" monomer and the dimer.

To explain the experimental findings, which indicated tighter dimer formation in the two mutant forms of rβA3, as compared to the wild-type protein, dissociation free energy changes were calculated for each protein (Table 3). The free energies were estimated for subunit exchange between the "closed" monomer and a dimer by the method suggested by Horton and Lewis (*41*). Interaction free energies and the corresponding rotation−translation energy losses for the dimer dissociation of rβA3, rβA3cp, and rβA3tr are shown in Table 3. Both mutant forms show higher solvation energy changes as compared to normal rβA3 as indicated by higher free energies of dissociation. Although there are minor differences between the calculated and the experimentally determined ΔG values (Table 3), the theoretical treatment correctly predicts that the two mutants proteins form tighter dimers than wild-type protein in the following order: rβA3tr > rβA3cp > rβA3 (Table 3). Hence, this approach is consistent with the analytical centrifugation data, which showed that both the loss of the N-terminal extension, and the replacement of the βA3 by γB interdomain linker, increases the tendency of rβA3 to associate into dimers.

DISCUSSION

On the basis of sedimentation equilibrium analysis, the subunit structure of rβA3-crystallin and the mutant forms rβA3tr and rβA3cp can be described as a reversible monomer−dimer system. Previous findings with murine rβA3 and βB2 (*44*), and the data shown herein, indicate that β-crystallins may under certain conditions be transiently monomeric. The lifetime of this state depends mainly on the protein concentration, predicting that βA3-crystallin is mostly monomeric at very low concentrations and predominantly dimeric at higher concentrations. This simple physical model also provides an explanation for subunit exchange during heterodimer formation (*44*, *45*), suggesting that subunit exchange proceeds through a transient monomeric state. Our present results differ slightly from previous data (*25*, *45*), which reported higher molecular masses of about 51 and 47 kDa for bovine βA3 and βA1, respectively. This discrepancy might be simply explained by the more rigorous reducing conditions we utilized in the sample preparation for centrifugation or actual differences in the dissociation constants for bovine and murine βA3-crystallins. As mentioned earlier, sample oxidation can lead to artifactual increases in molecular mass.

The terminal arms of β-crystallins appear to be cleaved as lens fiber cell age, and their specific cleavages may result from activation of the thiol proteinase m-calpain (*46*). Thiol proteases tend to cut between structural microdomains in the terminal extensions of βA3 from different species (*43*). However, in the lens, the effects of deletion of the amino-terminal extension on the associative behavior of the truncated protein is not clear. Using gel-filtration, rβA3tr elutes as a monomer, consistent with earlier results (*26*). A variety of different column matrixes, including Superdex 75, Superose 12, Sephadex, and ACA34 were tested with similar results. In contrast, sedimentation equilibrium data suggest

that truncation of the whole amino-terminal arm actually increases the tendency of rβA3 to form dimers. The reason for this discrepancy, performed under the same reducing conditions, remains unclear. A simple explanation might be that due to removal of the N-terminal region the protein is somewhat sticky and interacts with the gel filtration media, thus retarding its elution. Another possibility is that truncation of the terminal extension might influence the stability of the bound water surrounding the protein. Truncation of terminal extensions and partial dehydration could decrease the molecular radius up to 30% (unpublished results). This would be manifest as a compacting of the protein structure resulting in a lower apparent molecular size as estimated by gel filtration. Regardless, we have included the gel filtration data for comparison with our earlier work (*26*, *28*).

Overall, our ultracentrifugation data clearly support the view that the loss of the N-terminal extension of rβA3 increases its affinity to associate. This finding has remained consistent and is independent of the protein isolation method and analysis conditions. Furthermore, curve fitting of the equilibrium data (using goodness of fit criteria) does not indicate the presence of irreversible high-order aggregates.

The linker peptide has been suggested to be a conformational determinant controlling protein association (*18*, *19*). Hence, mutant bovine βB2, in which residues 82 to 87 of the extended linker peptide were replaced with the corresponding residues of γB linker, was monomeric (*20*). Surprisingly, when the linker in γB was replaced with the linker of βB2, the mutant γB remained monomeric (*27*). The βB2 linker may inhibit domain association by introducing the bulky residue E87 at the dimer domain interface as previously suggested (*18*). However, substitution of the normal connecting peptide of βA3 by the γB linker actually increases dimerization, although the residue corresponding to E87 present in both βA3 and βB2 was replaced with a glycine (Table 1). This increased dimerization potential might be due to the greater conformational flexibility of the γB linker, resulting from the presence of glycine at position 87, which allows for a better (tighter) interdomain fit.

To explain the energetics of the monomer−dimer equilibrium and tighter binding of the mutant proteins, the 3-dimensional structures of the βA3 monomers and dimers were modeled, and dissociation free energy was estimated using those structures. Although the dissociation free energy function yields the correct order of relative energy changes between a wild type and two mutant proteins, the absolute values of the free energy changes are different when compared to observed values (Table 3). This suggests that the use of the solvation energy function alone does not fully describe domain binding and other energy terms (*47*) may be considered in the future.

Using the accessible area change in the protein interface due to a dimer formation and assuming 25 cal/Å^2 (*48*), we estimated that the hydrophobic energy change in rβA3 (rβA3tr) was 18.3 kcal/mol and in rβA3cp was 18.2 kcal/mol. The fact that the most of associative tendency of the βA3-crystallins could be explained by hydrophobic energy change (Table 3) indicates a process similar to the entropically driven association dominated by hydrophobic interaction (*49*, *50*). Indeed, our preliminary dissociation constant measurements at different temperatures for the rβA3tr mutant show that both enthalpy and entropy of association have positive signs that support the entropy-driven association of βA3-crystallins (data not shown).

In conclusion, our results indicate that rβA3 and the two variant forms (rβA3cp and rβA3tr) exist in solution in reversible monomer−dimer equilibrium. This explains the rapid subunit exchange between the various eye lens β-crystallins resulting in various heterocomplex formations. We have confirmed preliminary earlier work by showing that replacement of the interdomain peptide of rβA3 has little effect on dimer formation (*26*). As the rβA3tr was shown to form a tighter dimer as compared to rβA3, the loss of the amino-terminal extension increases rather than decreases its tendency to self-associate.

ACKNOWLEDGMENT

We are very grateful to Dr. B. K. Lee (National Cancer Institute, NIH) for valuable discussions on energy calculations. Authors are also thankful to the Center of Molecular Modeling at National Institutes of Health for using commercial molecular modeling software on network.

REFERENCES

1. Wistow, G. J., and Piatigorsky, J. (1988) *Annu. Rev. Biochem. 57*, 479−504.
2. Bloemendal, H., and de Jong, W. W. (1991) *Prog. Nucleic Acid Res Mol. Biol. 41*, 259−281.
3. Lubsen, N. H., Aarts, H. J. M., and Schoenmakers, J. G. G. (1988) *Prog. Biophys. Mol. Biol. 51*, 47−76.
4. Caspers, G. J., Leunissen, J. A., and de Jong, W. W. (1995) *J. Mol. Evol. 40*, 238−248.
5. Chambers, C., and Russell, P. (1991) *J. Biol. Chem. 266*, 6742−6746.
6. Cartier, M., Breitman, M. L., and Tsui, L. C. (1992) *Nat. Genet. 2*, 42−45.
7. Litt, M., Carrero-Valenzuela, R., LaMorticella, D. M., Schultz, D. W., Mitchell, T. N., Kramer, P., and Maumenee, I. H. (1997) *Hum. Mol. Genet. 6*, 665−668.
8. Klopp, N., Favor, J., Loster, J., Lutz, R. B., Neuhauser-Klaus, A., Prescott, A., Pretsch, W., Quinlan, R. A., Sandilands, A., Vrensen, G. F., and Graw, J. (1998) *Genomics 52*, 152−158.
9. Kannabiran, C., Rogan, P. K., Olmos, L., Basti, S., Rao, G. N., Kaiser-Kupfer, M., and Hejtmancik, J. F. (1998) *Molecular Vision 4*.
10. Graw, J. (1999) *Prog. Retinal Eye Res. 18*, 235−267.
11. Heon, E., Priston, M., Schorderet, D. F., Billingsley, G. D., Girard, P. O., Lubsen, N., and Munier, F. L. (1999) *Am. J. Hum. Genet. 65*, 1261−1267.
12. Ren, Z., Li, A., Shastry, B. S., Padma, T., Ayyagari, R., Scott, M. H., Parks, M. M., Kaiser-Kupfer, M., and Hejtmancik, J. F. (2000) *Hum. Genet. 106*, 531−537.
13. Stephan, D. A., Gillanders, E., Vanderveen, D., Freas-Lutz, D., Wistow, G., Baxevanis, A. D., Robbins, C. M., VanAuken, A., Quesenberry, M. I., Bailey-Wilson, J., Juo, S. H., Trent, J. M., Smith, L., and Brownstein, M. J. (1999) *Proc. Natl. Acad. Sci. U.S.A 96*, 1008−1012.
14. Kmoch, S., Asfaw, B., Bezouska, K., Brynda, J., Sedlacek, J., Filipec, M., and Elleder, M. (1999) *Am. J. Hum. Genet. 65*(4), A305.
15. Wistow, G. J., Turnell, B., Summers, L., Slingsby, C., Moss, D., Miller, L., Lindley, P., and Blundell, T. (1983) *J. Mol. Biol. 170*, 175−202.
16. Sergeev, Y. V., Chirgadze, Y. N., Mylvaganam, S. E., Driessen, H., Slingsby, C., and Blundell, T. L. (1988) *Proteins 4*, 137−147.
17. White, H. E., Driessen, H. P. C., Slingsby, C., Moss, D. S., and Lindley, P. F. (1989) *J. Mol. Biol. 207*, 217−235.
18. Bax, B., Lapatto, R., Nalini, V., Driessen, H., Lindley, P. F., Mahadevan, D., Blundell, T. L., and Slingsby, C. (1990) *Nature 347*, 776−780.

19. Lapatto, R., Nalini, V., Bax, B., Driessen, H., Lindley, P. F., Blundell, T. L., and Slingsby, C. (1991) *J. Mol. Biol. 222*, 1067−1083.
20. Mayr, E. M., Jaenicke, R., and Glockshuber, R. (1994) *J. Mol. Biol. 235*, 84−88.
21. Bax, B., and Slingsby, C. (1989) *J. Mol. Biol. 208*, 715−717.
22. Sergeev, Y. V., and Hejtmancik, J. F. (1997) In *Techniques in Protein Chemistry* (Marshak, D. R., Ed.) pp 817−826, Academic Press, New York.
23. Norledge, B. V., Mayr, E. M., Glockshuber, R., Bateman, O. A., Slingsby, C., Jaenicke, R., and Driessen, H. P. (1996) *Nat. Struct. Biol. 3*, 267−274.
24. Kroone, R. C., Elliott, G. S., Ferszt, A., Slingsby, C., Lubsen, N. H., and Schoenmakers, J. G. G. (1994) *Protein. Eng. 7*, 1395−1399.
25. Werten, P. J. L., Carver, J. A., Jaenicke, R., and de Jong, W. W. (1996) *Protein. Eng. 9*, 1021−1028.
26. Hope, J. N., Chen, H. C., and Hejtmancik, J. F. (1994) *Protein Eng. 7*, 445−451.
27. Trinkl, S., Glockshuber, R., and Jaenicke, R. (1994) *Protein Sci. 3*, 1392−1400.
28. Hope, J. N., Chen, H.-C., and Hejtmancik, J. F. (1994) *J. Biol. Chem. 269*, 21141−21145.
29. Laemmli, U. K. (1970) *Nature 227*, 680−685.
30. Towbin, H., Staehelin, T., and Gordon, J. (1979) *Proc. Natl. Acad. Sci. U.S.A. 76*, 4350−4354.
31. Cohn, E. J., and Edsall, J. T. (1943) *Proteins, Amino Acids and Peptides*, Van Nostrand-Reinhold, Princeton, NJ.
32. Laue, T. M., Shah, B. D., Ridgeway, T. M., and Pelletier, S. L. (1992) In *Analytical Ultracentrifugation in Biochemistry and Polymer Science* (Harding, S. E., Rowe, A. J., and Horton, J. C., Eds.) pp 90−125, Royal Society for Chemistry, Cambridge, United Kingdom.
33. Abola, E., Bernstein, F. C., Bryant, S. H., Koetzle, T. F., and Weng, J. (1987) in *Crystallographic Databases-Information Contene, Software Systems, Scientific Applications* (Allen, F. H., Bergerhoff, G., and Sievers, R., Eds.) pp 107−132, Data Comission of the International Union of Crystallography, Cambridge.
34. van Rens, G., de Jong W., and Bloemendal, H. (1992) *Mol. Biol. Rep. 16*, 1−10.
35. Needleman, S. B., and Wunsch, C. D. (1970) *J. Mol. Biol. 48*, 443−453.
36. Levitt, M. (1992) *J. Mol. Biol. 226*, 507−533.
37. Lee, C. (1994) *J. Mol. Biol. 236*, 918−939.
38. Laskowski, R. A., MacArthur, M. W., Moss, D. S., and Thornton, J. M. (1993) *J. Appl. Crystallogr. 26*, 283−291.
39. Eisenberg, D., and McLachlan, A. D. (1986) *Nature 319*, 199−203.
40. Richmond, T. J. (1984) *J. Mol. Biol. 178*, 63−89.
41. Horton, N., and Lewis, M. (1992) *Protein Sci. 1*, 169−181.
42. Erickson, H. P. (1989) *J. Mol. Biol. 206*, 465−474.
43. Sergeev, Y. V., David, L. L., Chen, H.-C., Hope, J. N., and Hejtmancik, J. F. (1998) *Mol. Vision 4*.
44. Hejtmancik, J. F., Wingfield, P., Chambers, C., Russell, P., Chen, H.-C., Sergeev, Y. V., and Hope, J. N. (1997) *Protein Eng. 10*, 1347−1352.
45. Werten, P. J., Lindner, R. A., Carver, J. A., and de Jong, W. W. (1999) *Biochim. Biophys. Acta 1432*, 286−292.
46. David, L. L. and Shearer, T. R. (1993) *FEBS Lett. 324*, 265−270.
47. Gilson, M. K., Given, J. A., Bush, B. L., and McCammon, J. A. (1997) *Biophys. J. 72*, 1047−1069.
48. Chothia, C., and Janin J. (1975) *Nature 256*, 705−708.
49. Ross P. D., and Subramanian S. (1981) *Biochemistry. 20* 3096−3102.
50. Sackett D. L., and Lippoldt R. E. (1991) *Biochemistry 30*, 3511−3517.

BI001882H